BRL R 1357

BRL

REPORT NO. 1357

THE DYNAMIC EXPANSION OF A SPHERICAL CAVITY IN AN ELASTIC-PERFECTLY-PLASTIC MATERIAL

by

Chi-Hung Mok

February 1967

U. S. ARMY MATERIEL COMMAND
BALLISTIC RESEARCH LABORATORIES
ABERDEEN PROVING GROUND, MARYLAND

Destroy this report when it is no longer needed.
Do not return it to the originator.

The findings in this report are not to be construed as an official Department of the Army position, unless so designated by other authorized documents.

B A L L I S T I C R E S E A R C H L A B O R A T O R I E S

REPORT NO. 1357

FEBRUARY 1967

THE DYNAMIC EXPANSION OF A SPHERICAL CAVITY IN AN ELASTIC-PERFECTLY-PLASTIC MATERIAL

Chi-Hung Mok

Exterior Ballistics Laboratory

RDT&E Project No. 1P222901A201

A B E R D E E N P R O V I N G G R O U N D, M A R Y L A N D

B A L L I S T I C R E S E A R C H L A B O R A T O R I E S

REPORT NO. 1357

CHMok/cr
Aberdeen Proving Ground, Md.
February 1967

THE DYNAMIC EXPANSION OF A SPHERICAL CAVITY IN AN ELASTIC-PERFECTLY-PLASTIC MATERIAL

ABSTRACT

It has been shown that a finite-difference numerical technique can be used to solve mixed initial-and boundary-value problems involving high-speed elastic-plastic flow with spherical symmetry. Numerical solutions for the dynamic expansion of a spherical cavity under a constant pressure are presented to demonstrate the nature and capability of the numerical scheme. The solution for an elastic material agrees closely with the exact solution. The solution for an elastic-perfectly-plastic material has confirmed Green's prediction concerning the motion of the elastic-plastic boundary. At large times, the asymptotic solution of the dynamic problem is different from the quasi-static solution. This result indicates that the quasi-static approximation may not hold in dynamic plasticity. A non-linear dependence of the plastic solution on the boundary condition is also observed in the results.

TABLE OF CONTENTS

1. INTRODUCTION

The problem of high-speed elastic-plastic flow with spherical symmetry is of interest for two reasons. First, it has practical application in underground explosions and in the detonation of high-explosives in solids; secondly, with little increase in the mathematical difficulties from the uniaxial flow, the simple geometry of this problem allows the study of an elastic-plastic flow involving the bi-axial state of stresses and inertia forces. Perhaps this second characteristic is equally interesting to both an applied mathematician and an experimentalist who is concerned with obtaining information of the dynamic yield properties of a material under bi-axial state of stresses. In the past, many authors have investigated this problem; the reader may refer to a paper by Hopkins[1*] for a general review on the current status of research in this subject. Most of the published work is concerned with small deformations. The materials investigated include the idealized elastic-perfectly-plastic and elastic-linear-work-hardening materials. However, up to present, because of the mathematical difficulties involved in treating two-phase flows, there existed no analytical solution which describes satisfactorily all the phases of the impact process. As pointed out in Section 2 below, only at the very beginning of an impact is the location of the elastic-plastic boundary known and a simple analytic description of the flow available. However, for the major duration of the impact process, the description of the flow seems to rely upon a numerical solution. The purpose of this report is to show that this problem can be solved for various initial and boundary conditions by using a finite difference technique. The elastic-plastic solution obtained for the expansion of a spherical cavity under constant internal pressure has demonstrated some interesting facts concerning the impact phenomena. It has confirmed Green's[1,2] results regarding the motion of the elastic-plastic boundary and also has exhibited the inadequacy of the quasi-static approximation

Superscript numbers denote references which may be found on page 30.

in dynamic plasticity. Numerical solutions of spherical elastic-plastic flow have also been obtained by Davids et al[3] and by Friedman et al.[4]

2. BASIC EQUATIONS

Referring to a spherical coordinate system, r, θ and ϕ, with the origin at the center of the cavity, only the equation of motion in the r direction will not vanish identically because of the spherical symmetry considered here; hence,

$$\frac{\partial \sigma_r}{\partial r} + 2\,\frac{\sigma_r - \sigma_\theta}{r} = \rho\,\frac{\partial v}{\partial t} \quad . \tag{1}$$

In the equation, r is the Lagrangian position of a particle; ρ is the mass density of the material in the underformed state; v the radial velocity of the particle, and σ_r and σ_θ are respectively the normal stress components in the radial and the circumferential directions. The stresses are engineering stresses calculated with reference to the undeformed state. This report considers only small deformations; hence, differences between the engineering and true values of stress and strain will be negligible.

The material is considered to be elastic, perfectly plastic with a constant yield stress σ_o in both simple compression and tension. Both von Mises and Tresca yield conditions reduce to the form[5]

$$\sigma_r - \sigma_\theta = \pm\,\sigma_o \quad . \tag{2}$$

The material will deform plastically when this equation is satisfied and when

$$(\sigma_r - \sigma_\theta)\,(\dot{\sigma}_r - \dot{\sigma}_\theta) = 0 \quad . \tag{3}$$

Otherwise, when

$$|\sigma_r - \sigma_\theta| < \sigma_o \quad , \tag{4}$$

or when

$$\sigma_r - \sigma_\theta = \pm \sigma_o$$

but (5)

$$(\sigma_r - \sigma_\theta)\ (\dot{\sigma}_r - \dot{\sigma}_\theta) < 0 \ ,$$

the material behaves as an elastic body.

For the elastic regime, the material obeys Hooke's law. Expressing the radial and circumferential strains, ε_r and ε_θ respectively, in terms of the radial displacement u,

$$\varepsilon_r = \frac{\partial u}{\partial r}$$

$$\varepsilon_\theta = \frac{u}{r} \quad , \tag{6}$$

Hooke's law in a differential form can be written as

$$\frac{\partial \sigma_r}{\partial t} - 2\nu \frac{\partial \sigma_\theta}{\partial t} - E \frac{\partial v}{\partial r} = 0$$

$$\nu \frac{\partial \sigma_r}{\partial t} - (1 - \nu) \frac{\partial \sigma_\theta}{\partial t} + \frac{E}{r} v = 0 \quad . \tag{7}$$

These two equations and the equation of motion, Equation (1), must be solved simultaneously to obtain the elastic solution.

For most materials, under moderate pressures, no appreciable plastic volume change will occur. Hence, the elastic relation between the mean hydrostatic stress, $(\sigma_r + 2\sigma_\theta)/3$ and the dilatation $\partial u/\partial r + 2u/r$

can be used for describing the plastic flow. Using Hooke's law and relating σ_r to σ_θ by the yield condition, the relation expressed in a differential form is

$$\frac{1 - 2\nu}{E} \frac{\partial \sigma_r}{\partial t} - 1/3 \frac{\partial v}{\partial r} - 2/3 \frac{v}{r} = 0 \ . \tag{8}$$

This equation must be solved simultaneously with the yield condition, Equation (2), and the equation of motion, Equation (1), to provide results for the plastic flow.

A convenient representation of the solutions of these equations can be obtained by introducing the following dimensionless variables,

$$x = \frac{r}{r_o}$$

$$R = \frac{\sigma_r}{\sigma_o}$$

$$\Theta = \frac{\sigma_\theta}{\sigma_o}$$

$$\bar{\sigma} = \frac{\sigma_o}{E} \qquad (9)$$

$$\tau = \frac{c_d t}{r_o}$$

and

$$V = \frac{v}{c_d \bar{\sigma}}$$

where r_o is the radius of the cavity and $c_d = [(1 - \nu)(E/\rho)/(1 - \nu - 2\nu^2)]^{1/2}$ is the dilatational wave speed in an elastic solid. In terms of these dimensionless variables, the simultaneous partial differential equations for the dynamic problem are

$$\frac{\partial R}{\partial x} - \frac{1-\nu}{1-\nu-2\nu^2}\frac{\partial V}{\partial \tau} + \frac{2}{x}(R - \Theta) = 0$$

$$\frac{\partial R}{\partial \tau} - 2\nu \frac{\partial \Theta}{\partial \tau} - \frac{\partial V}{\partial x} = 0 \qquad (10)$$

$$\nu\frac{\partial R}{\partial \tau} - (1 - \nu)\frac{\partial \Theta}{\partial \tau} + \frac{1}{x} V = 0$$

and

$$\frac{\partial R}{\partial x} - \frac{1-\nu}{1-\nu-2\nu^2}\frac{\partial V}{\partial \tau} \pm \frac{2}{x} = 0$$

$$(1 - 2\nu)\frac{\partial R}{\partial \tau} - \frac{1}{3}\frac{\partial V}{\partial x} - \frac{2}{3}\frac{V}{x} = 0 \qquad (11)$$

$$\Theta = R \pm 1 \quad .$$

Equation (10) will apply for elastic deformation; i.e., when

$$|R - \Theta| < 1 \qquad (12)$$

or when

$$R - \Theta = \pm 1 \qquad (13)$$

but

$$(R - \Theta)\,(\dot{R} - \dot{\Theta}) < 1 \quad .$$

Equation (11) will hold for the plastic flow, when

$$R - \Theta = \pm 1$$

and

$$(R - \Theta)\,(\dot{R} - \dot{\Theta}) = 0 \quad . \qquad (14)$$

The $\pm$ signs are for the situations when $R - \Theta = \pm 1$ respectively.

In Equations (10) and (11), only one parameter, the Poisson's ratio ν appears in the coefficients. The equations written in this form provide a clearer picture of the dependence of the solution on various parameters of material properties. For a stress boundary condition, the stress distribution around a plastically deformed cavity at any instant depends only on the Poisson's ratio and the ratio between the applied pressure to the yield stress of the material.

Equations (10) and (11) are two sets of first order linear hyperbolic partial differential equations. Their solutions can be obtained by combining two waves associating with a displacement function as described

by Hunter.[6] However, this method requires *a priori* a knowledge of the position of the boundary of the elastic and plastic regions of the material which can be obtained only in few instances. Green,[1,2] has proved that when there is a discontinuity in the magnitude of the radial strain ε_r across the elastic-plastic boundary, the boundary will travel with a constant velocity $c_p = [E/3\,\rho\,(1 - 2\nu)]^{1/2}$, and the position of the boundary is, therefore, known. However, with the rapid attentuation of a diverging spherical wave, this discontinuity in radial strain can be maintained only near the very beginning of an impact. Therefore, other techniques must be used to obtain the solution which holds for the major portion of the impact.

3. NUMERICAL SCHEMES

In this report, a finite difference scheme proposed by Lax[7] will be used to obtain a solution of the equations derived above. The original scheme has been shown suitable for solving initial value problems of hyperbolic partial differential equations in hydrodynamics. The scheme is extended here for mixed boundary-and initial-value problems with regions of solutions governed by different sets of equations. The results obtained using this scheme are compared with known analytical solutions for the case of elastic waves. The accuracy of the numerical results appears to be satisfactory. An appendix to this report describes the computer program used to obtain the present results.

The finite difference scheme is for any set of partial differential equations assuming the conservation form; i.e.,

$$\frac{\partial F}{\partial x} + \frac{\partial G}{\partial \tau} + H = 0 \ , \tag{15}$$

where F, G and H are functions of the dependent and independent variables. The numerical scheme replaces $\partial F/\partial x$ by a central difference quotient; i.e.,

$$\frac{F_{n+1,k} - F_{n-1,k}}{2\Delta x} \tag{16}$$

where Δx denotes an increment in x; $F_{n+1,k}$ designates the value of F at the grid point located at distances $(n+1)\ \Delta x$ and $k\Delta\tau$ from the origin in the x and τ plane. The time derivative $\partial G/\partial\tau$ is substituted by a forward difference quotient,

$$\frac{G_{n,\,k+1} - \frac{1}{2}(G_{n+1,k} + G_{n-1,k})}{\Delta\tau} \tag{17}$$

Finally, the function H is replaced by the average value at two neighboring grid points at the time $k\Delta\tau$,

$$\frac{1}{2}(H_{n+1,k} + H_{n-1,k}) \tag{18}$$

The scheme is equivalent to adding into the original equation a term which is due to an artifical viscosity of the magnitude of $(\Delta x)^2/2\Delta\tau$. The stability and convergence of this scheme has been discussed by Lax.[7] The stability criterion is similar to the Courant-Friedrichs-Lewy condition, i.e., $\Delta\tau/\Delta x<c$ where c is a quantity which may depend on the variables in the problem.

The present equations, Equations (10) and (11), are in the conservative form and, hence, can be solved numerically with this method. As an example, the finite difference equation for the first equation of (10) is obtained; i.e.,

$$\frac{R_{n+1,k} - R_{n-1,k}}{2\Delta x} - \frac{1-\nu}{1-\nu-2\nu^2}\,\frac{V_{n,k+1} - \frac{1}{2}\,(V_{n+1,k} + V_{n-1,k})}{\Delta\tau}$$

$$+ \frac{R_{n+1,k} - \Theta_{n+1,k}}{x_{n+1,k}} + \frac{R_{n-1,k} - \Theta_{n-1,k}}{x_{n-1,k}} = 0\ .$$

After being converted to finite difference equations, the three equations in (10) and in (11) will provide three algebraic equations sufficient for solving the values of the dependent variables at $\tau = (k+1)\Delta\tau$;

namely, $R_{n,k+1}$, $V_{n,k+1}$ and $\Theta_{n,k+1}$ from the known data at a previous time $k\Delta\tau$; namely, $R_{n-1,k}$, $\Theta_{n+1,k}$, $\Theta_{n-1,k}$, $V_{n+1,k}$ and $V_{n-1,k}$. At each point, the finite difference equations for elastic deformations, Equation (10), will be first used to obtain $R_{n,k+1}$ and $\Theta_{n,k+1}$. If the difference between them $|R_{n,k+1} - \Theta_{n,k+1}|$ is greater than unity, then the calculations will be revised by using the finite difference equations for plastic flow which are derived from Equations (11).

The above scheme can be applied very conveniently at points other than those on the boundary. However, when the central point x_n is on the cavity surface, the point $x_{n-1,k}$ will be outside the body, and fictitious values must be assigned for the dependent variables at this point in order to use the Lax numerical schemes. The present investigation shows that, for this situation, satisfactory results can be obtained by using a different numerical scheme. In the new scheme, the Lax method is applied in reverse to those dependent variables whose values are not specified on the boundary. Accordingly, a central difference formula is used for the time derivative and a forward difference formula for the space derivative. As an example, the space and time derivatives for the dependent variable V are

$$\frac{\partial V}{\partial \tau} = \frac{V_{n,k+1} - V_{n,k+1}}{2\Delta\tau}$$
$$\frac{\partial V}{\partial x} = \frac{V_{n+1,k} - \frac{1}{2}(V_{n,k+1} + V_{n,k-1})}{\Delta x} \quad . \tag{19}$$

However, for the derivatives of the dependent variables whose values are specified on the boundary, R in this case, the Lax scheme is kept. As a result, a fictitious value $R_{n-1,k}$ must be assumed, which, together with the other two unknowns $V_{n,k+1}$ and $\Theta_{n,k+1}$, can be obtained from the three finite-difference equations derived from Equations (10) or Equation (11)

using Equation (19). One of the unknowns in the calculation at an interior point, $R_{n,k+1}$ is now a known quantity which has the specified value of R on the boundary at $\tau = (k + 1)\Delta\tau$.

4. RESULTS FOR ELASTIC CASE - ACCURACY OF THE NUMERICAL SCHEME

The case of a constant pressure applied suddenly on the surface of a spherical cavity within an infinite elastic solid is studied to demonstrate the capability of the numerical scheme. In Figures 1a and 1b, the principal shear stress in the present numerical results is compared to those obtained analytically by Hunter[8] and numerically by Chou.[9] Chou uses the method of characteristics in obtaining his solution. Considering the rather large grid size (twenty-five points per cavity radius) used to obtain the present solution, the agreement between this solution and the other solutions is satisfactory.

However, near the elastic wave front where a jump in the values of the shear stress exists, a large discrepancy is observed between this solution and the exact one. The discrepancy is mainly due to the artificial viscosity which is associated with the numerical scheme and tends to smooth the sharp discontinuities of the solution. Since the artificial viscosity is equal to $(1/2)\ (\Delta x)^2/\Delta\tau$, the effects can be greatly reduced by increasing the ratio of $\Delta\tau/\Delta x$, as indicated by comparing the results obtained with $\Delta\tau/\Delta x = 1$ and 1/2. For this case, $\Delta x/\Delta\tau = 1$ is the maximum value allowed by the stability criterion; at this $\Delta x/\Delta\tau$ ratio some small oscillations in the solution which are not shown in the figures have already occurred near the wave front. The effects of the viscosity can also be reduced by diminishing the grid size as seen in the results for $\Delta x = 0.01$ and 0.02. However, considering the increase of computing time, the second method of reducing viscosity is not as efficient as the first one. Roberts[10] has proposed a much more effective method for improving the accuracy of this numerical scheme. The technique involves combining several solutions of first order accuracy obtained with a fixed $\Delta x/\Delta\tau$ ratio. Solutions with accuracy of order greater than one can be obtained very easily.

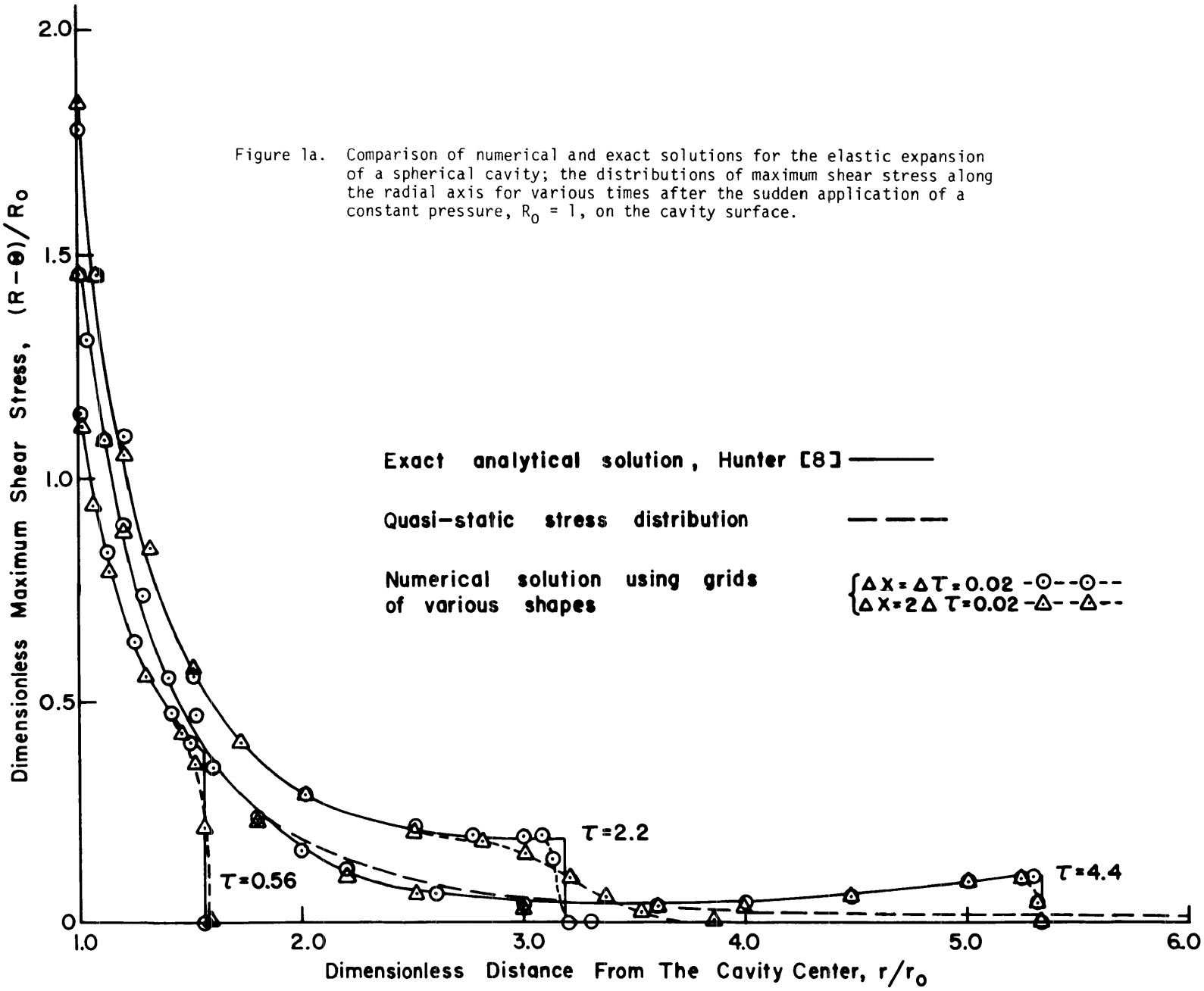

Figure 1a. Comparison of numerical and exact solutions for the elastic expansion of a spherical cavity; the distributions of maximum shear stress along the radial axis for various times after the sudden application of a constant pressure, $R_0 = 1$, on the cavity surface.

Figure 1b. Comparison of numerical and exact solutions for the elastic expansion of a spherical cavity; the variation of maximum shear stress at the cavity surface after the sudden application a constant pressure, $R_o = 1$, on the surface.

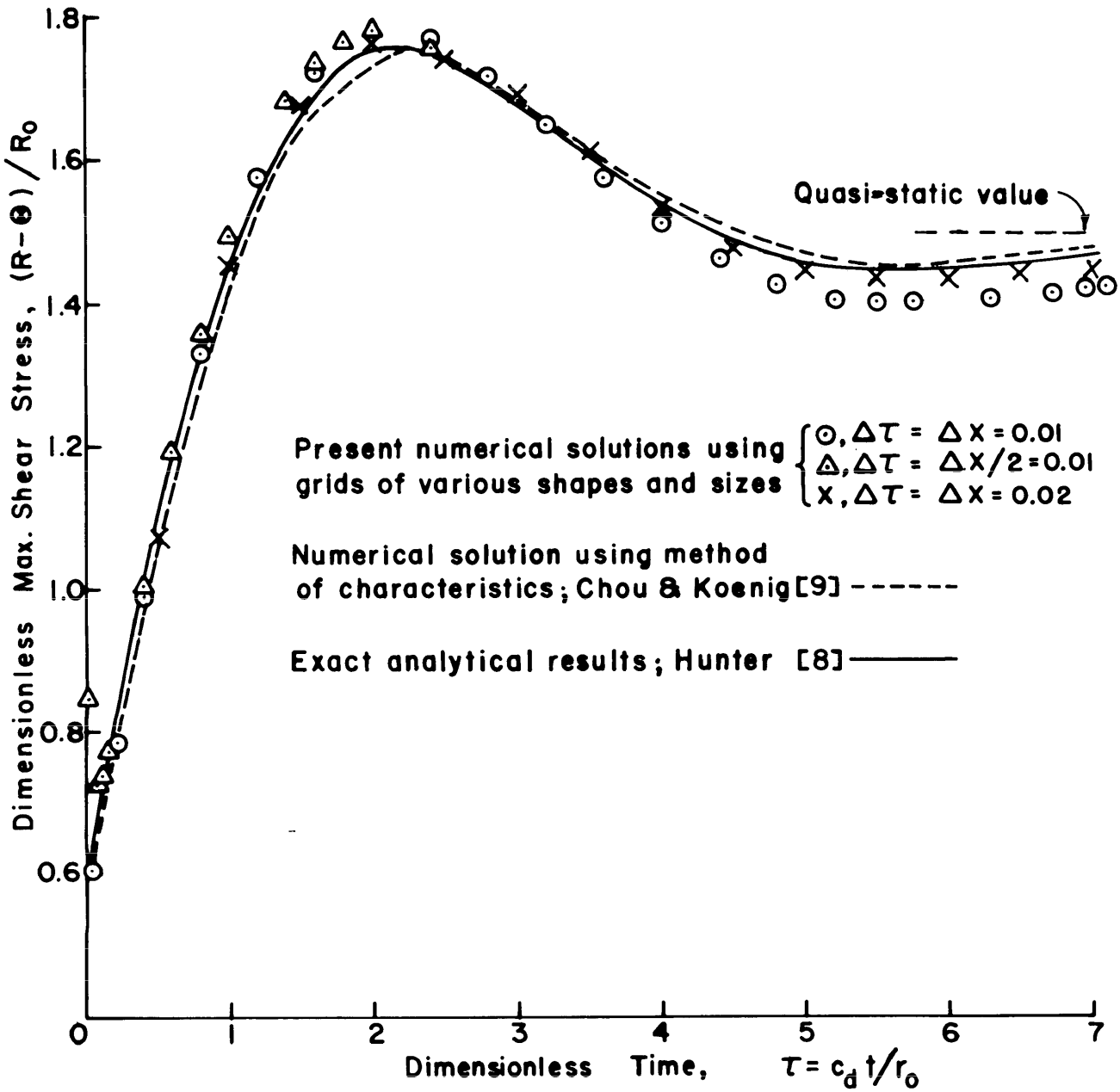

5. RESULTS FOR ELASTIC-PERFECTLY-PLASTIC MATERIAL

The numerical scheme just discussed has also been used to obtain the elastic-perfectly-plastic solution for a spherical cavity expanded under a constant internal pressure which is suddenly applied at $\tau = 0$. Typical sets of results are shown in Figures 2a through 3b for the cases in which the magnitudes of the internal pressures are 2 and 20 times of the constant yield stress of the material. In the results for the latter case, the evidence of two discontinuities can be seen in the profiles of stresses along the radial axis. The one which is farther away from the cavity surface is the elastic wave front while the one propagating behind is the plastic wave front which separates the regions of plastic and elastic deformation. The constant speed of propagation of the elastic wave front agrees closely with the exact value of the dilatation wave speed, c_d obtained here. The magnitude of the jump in the dependent variables across the elastic wave front also seems to agree with the exact solution which is represented by the dashed curves in Figures 2a to 2c.

The elastic-plastic boundary moves at a constant speed when a discontinuity in the radial stress across the boundary is visible near the beginning of the impact. The value of the speed agrees with the theoretical one predicted by Green,[1] namely, $c_p = [E/3\rho(1 - 2\nu)]^{1/2}$. This result is shown in Figure 4 in which the position of the elastic-plastic boundary at all times is plotted. Figure 4 also indicates that, for the present boundary condition, the movement of the elastic-plastic boundary will slow down as the discontinuity across the boundary disappears because of the geometrical dispersion. As long as the pressure on the cavity surface remains unchanged, the motion of the elastic-plastic boundary will come to a halt and then reverse its direction towards the cavity surface. This result is quite different from that observed in the static solution for the same elastic-plastic problem; when the constant pressure is applied quasi-statically at the boundary, a plastic zone next to the cavity surface is always maintained by the

Figure 2a. Numerical results for the elastic-plastic expansion of a spherical cavity; the distributions of radial stress along the radial axis for various times after the sudden application of a constant pressure, $R_0 = 2$, on the cavity surface. Arrows indicate the positions of the elastic-plastic boundary.

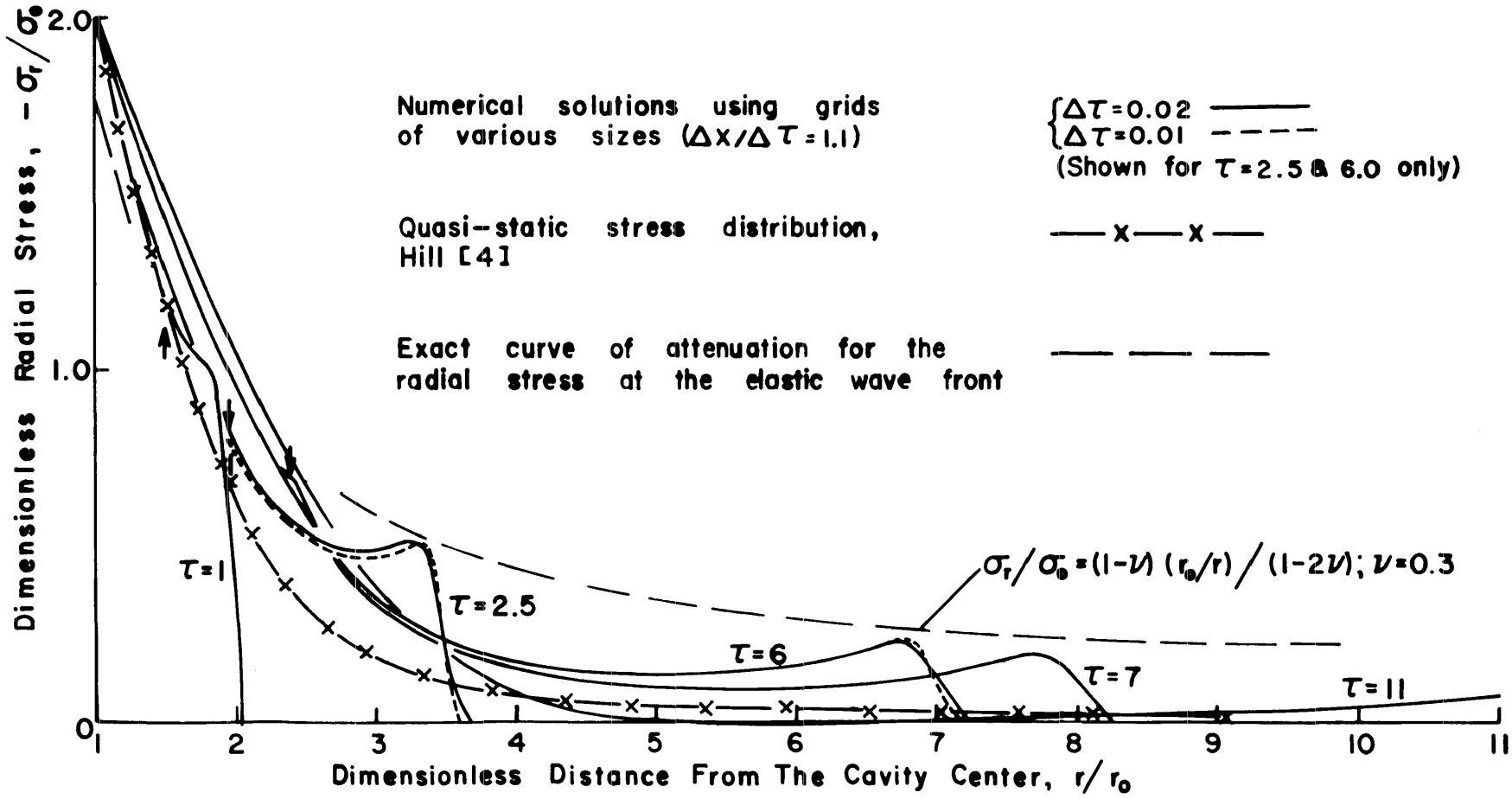

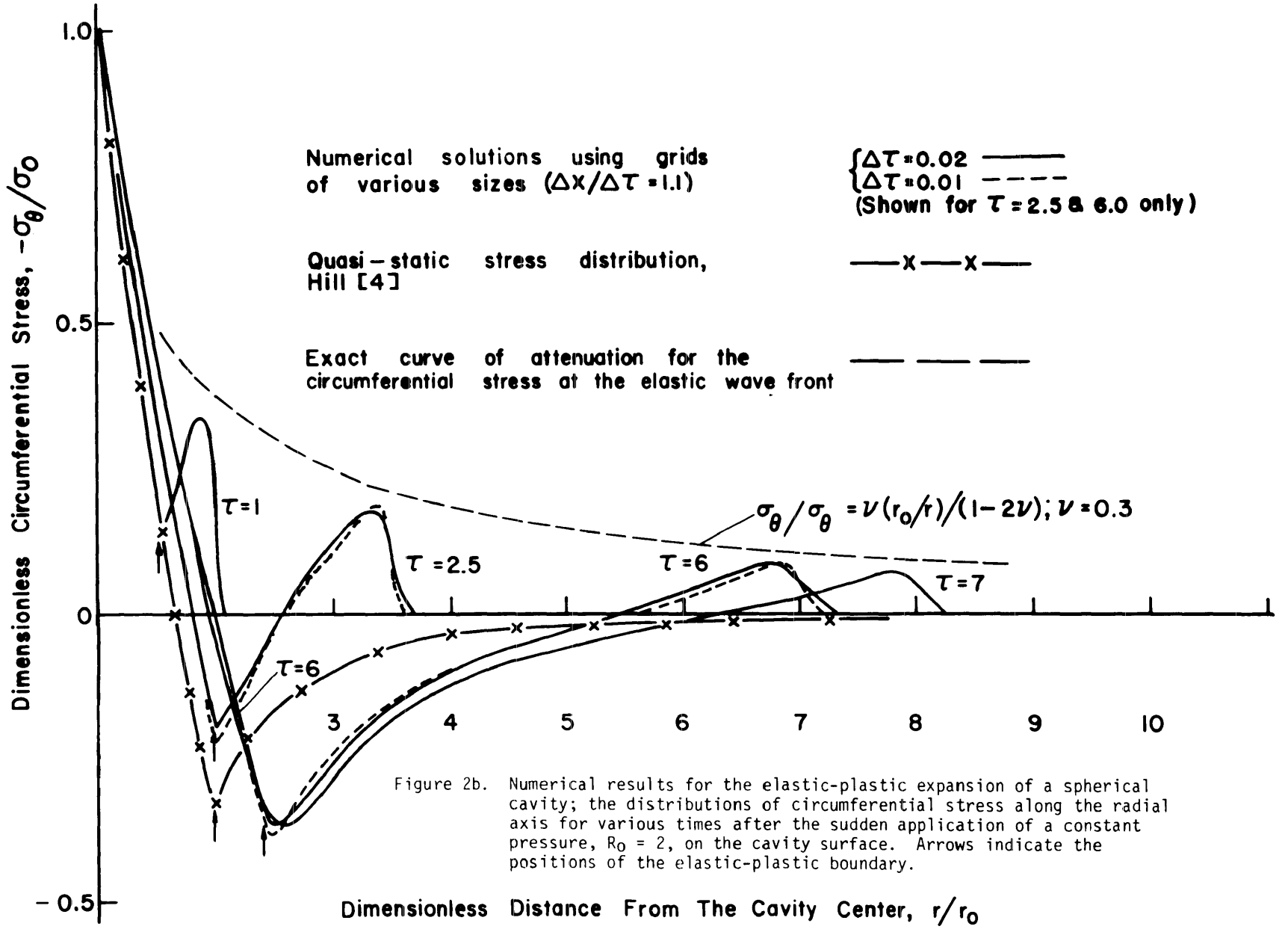

Figure 2b. Numerical results for the elastic-plastic expansion of a spherical cavity; the distributions of circumferential stress along the radial axis for various times after the sudden application of a constant pressure, $R_0 = 2$, on the cavity surface. Arrows indicate the positions of the elastic-plastic boundary.

Figure 2c. Numerical results for the elastic-plastic expansion of a spherical cavity; the distributions of particle velocity along the radial axis for various times after the sudden application of a constant pressure, $R_0 = 2$, on the cavity surface. Arrows indicate the positions of the elastic-plastic boundary.

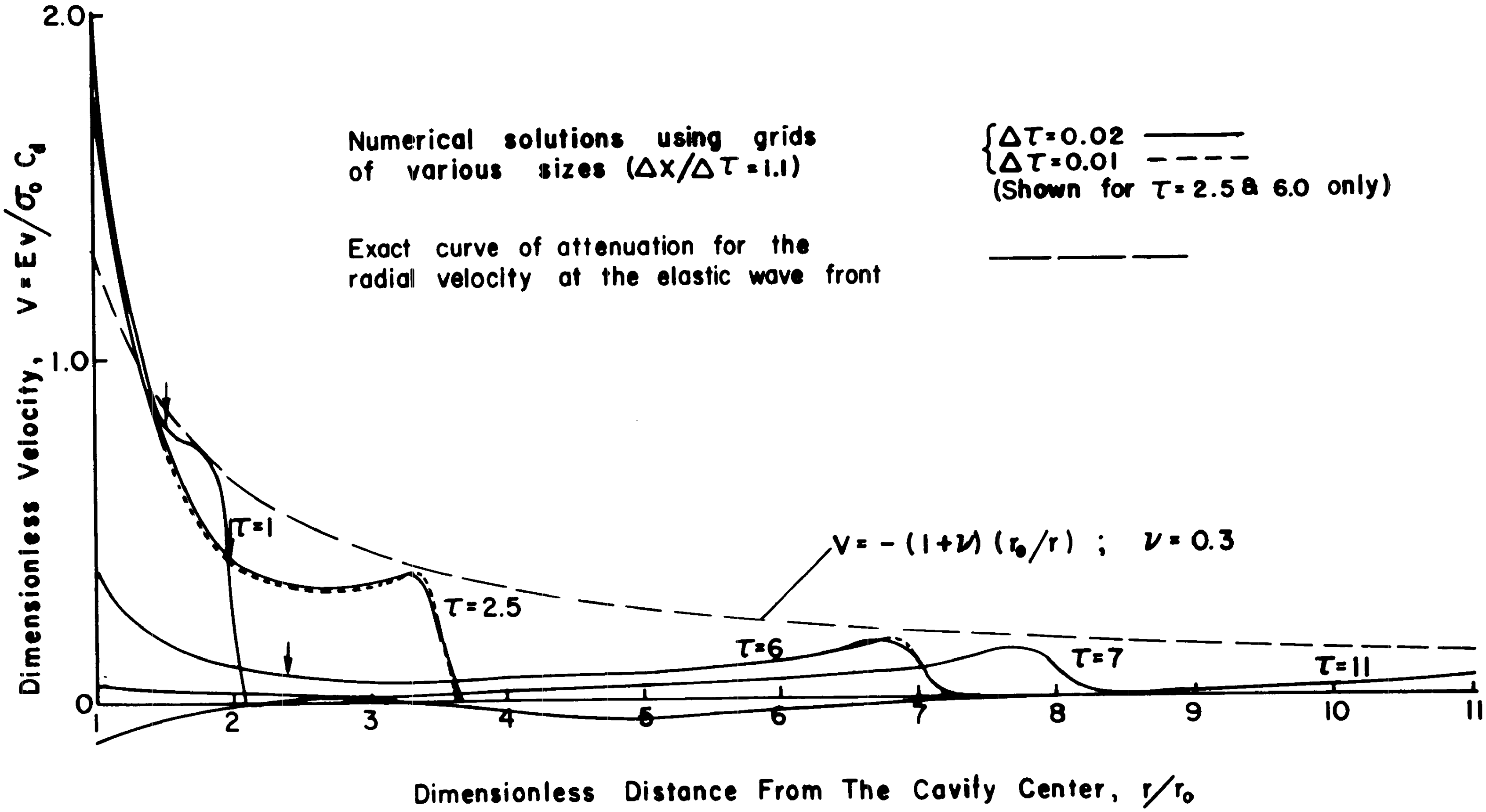

Figure 2d. Numerical results for the elastic-plastic expansion of a spherical cavity; the distributions of radial displacement along the radial axis for various times after the sudden application of a constant pressure, $R_0 = 2$, on the cavity surface. Arrows indicate the positions of the elastic-plastic boundary.

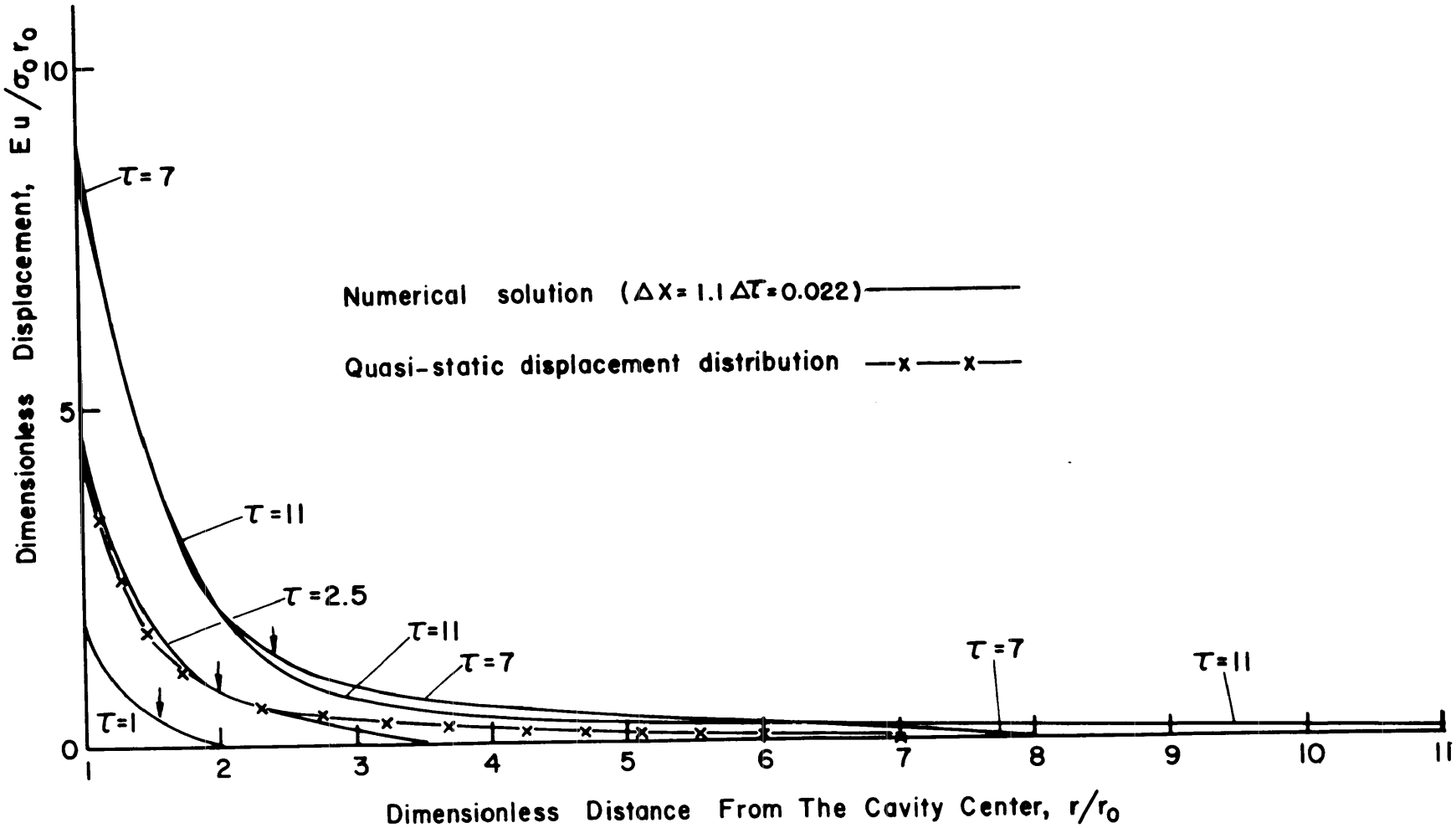

Figure 3a. Numerical results for the elastic-plastic expansion of a spherical cavity; the distributions of radial stress along the radial axis for several times after the sudden application of a constant pressure, $R_0 = 20$, on the cavity surface. AArrows indicate the positions of the elastic-plastic boundary.

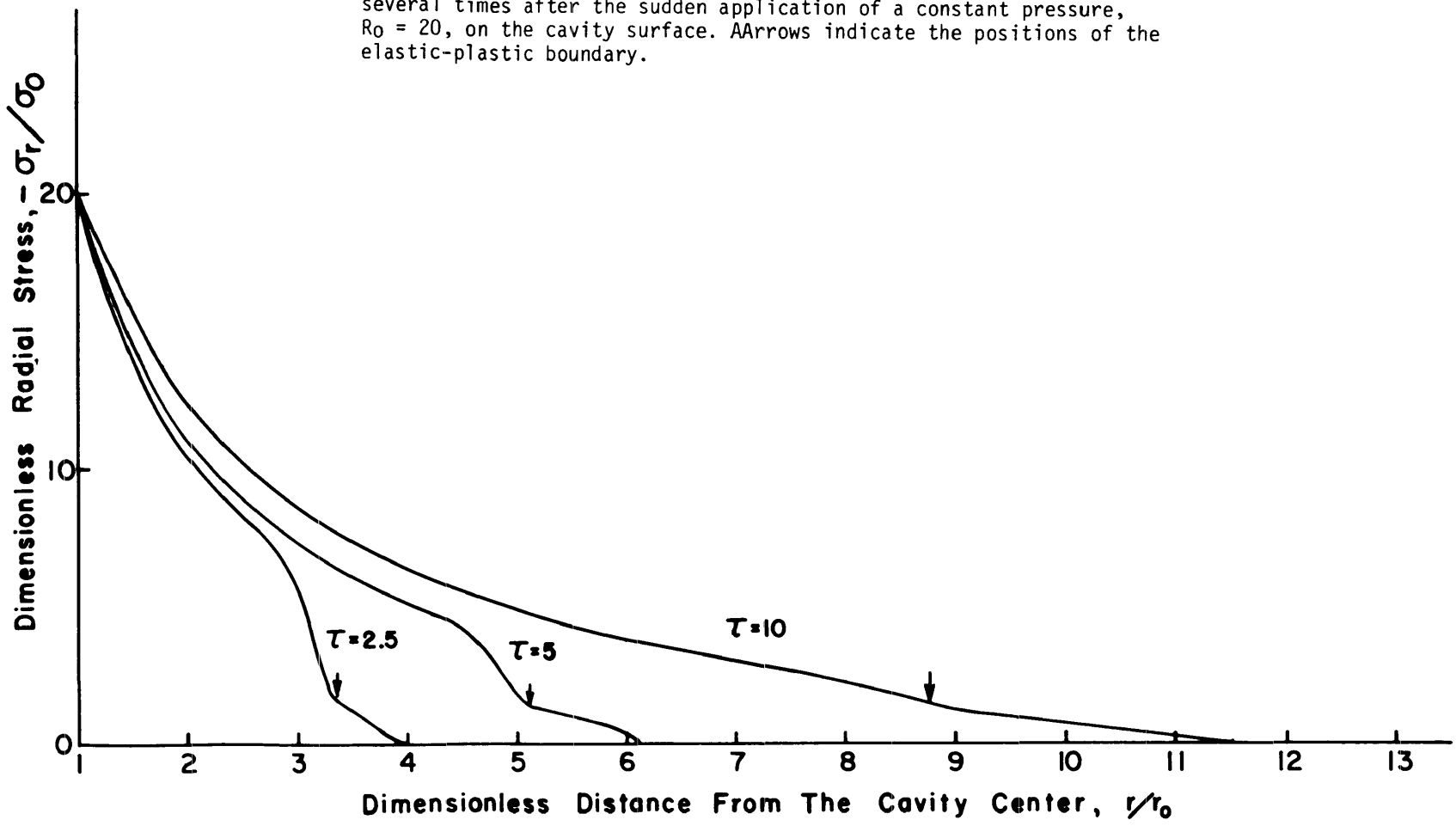

Figure 3b. Numerical results for the elastic-plastic expansion of a spherical cavity; the distributions of circumferential stress along the radial axis for several times after the sudden application of a constant pressure, $R_0 = 20$, on the cavity surface. Arrows indicate the positions of the elastic-plastic boundary.

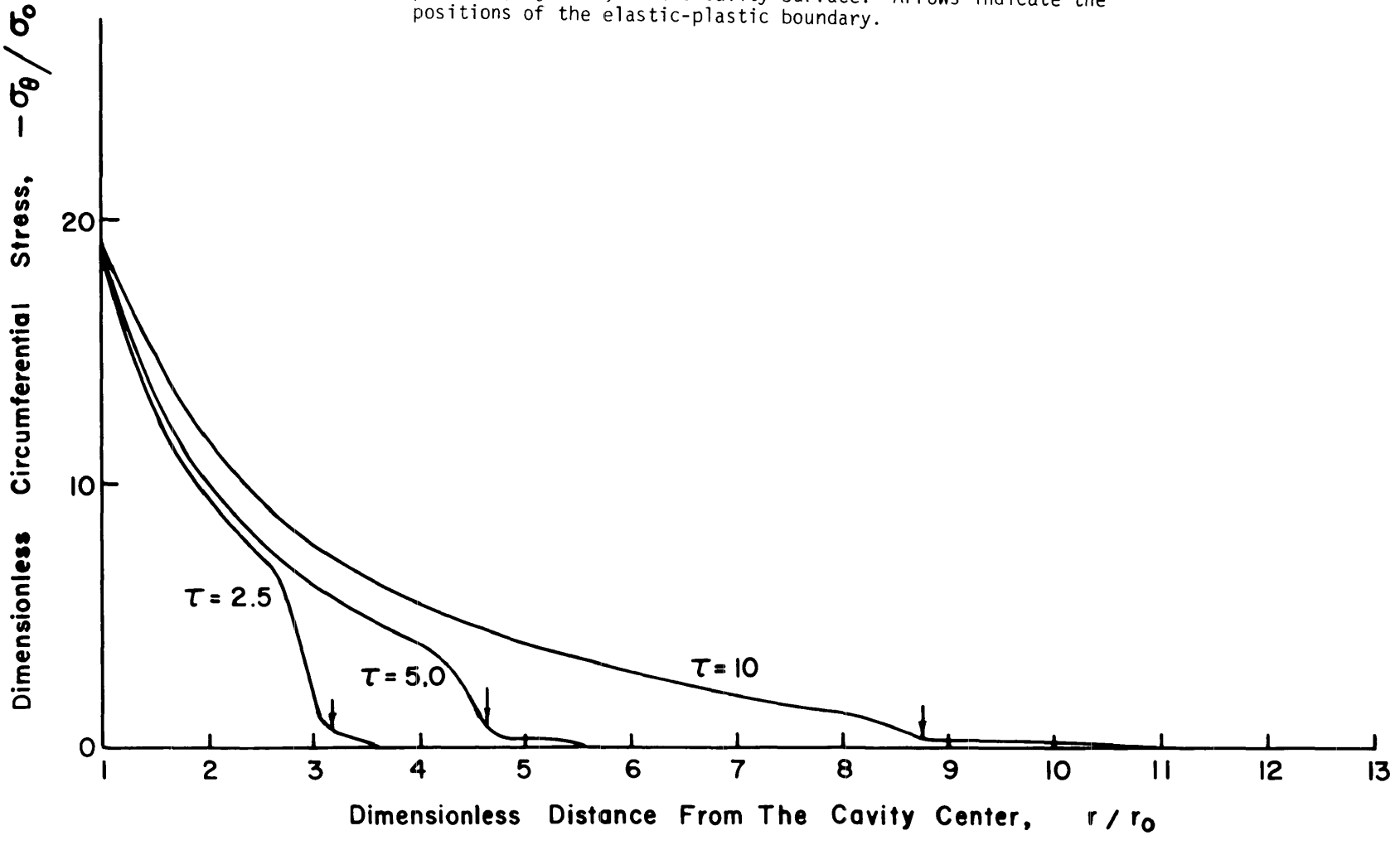

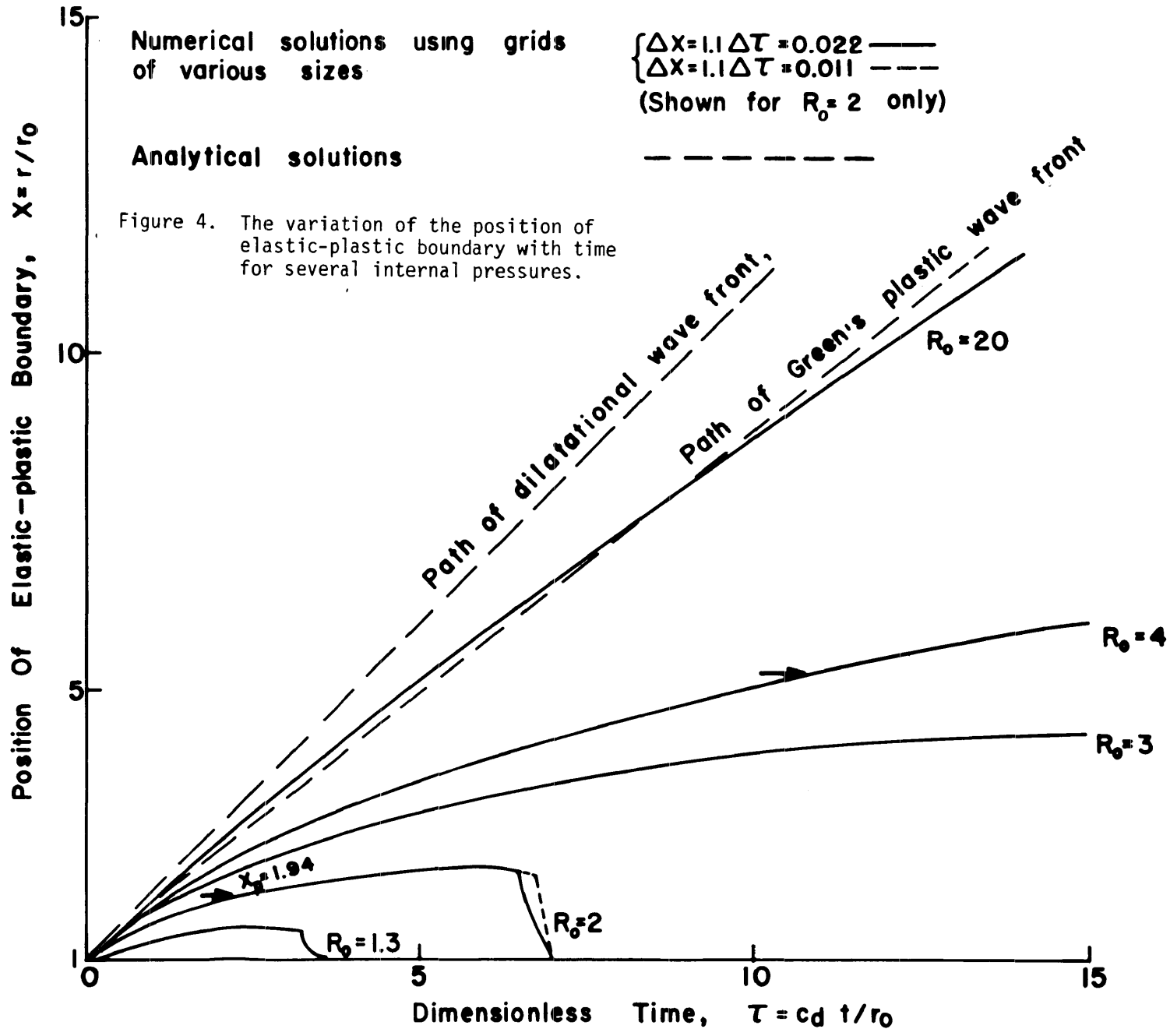

Figure 4. The variation of the position of elastic-plastic boundary with time for several internal pressures.

applied pressure.[5] Differences between the static solutions and the asymptotic dynamic solution at large times can also be observed in the distributions of the stresses and displacements along the radial axis (Figures 2a to 2d). A larger deformation and a higher radial stress occur in the dynamic case than do in the static case. These differences are not likely to be attributable to errors in the numerical solution, because the comparison of the results obtained with two grid sizes does not suggest the possible existence of such large differences in the solution (Figure 2a). The maximum radius of the elastic-plastic boundary is also larger in the dynamic case than in the static case. These disagreements between the dynamic solution at a large time and the static solution are probably due to the residual stresses produced by the inertial force occurring in the dynamic deformation process. This result implies that, in some circumstances, the quasi-static approximation may not be valid in dynamic plasticity. The quasi-static approximation in which the static solution of a problem is used to describe the long-time behavior of the dynamic solution holds in many situations in dynamic elasticity.[8,11,12]

Figures 4 and 5 show, for all times, the dependence of the particle velocity and of the position of the elastic-plastic boundary on the magnitude of the applied pressure. Although all of the results for various applied pressure seem to be similar qualitatively, the magnitudes of various parameters in the solution seems to be quite sensitive to a change in the pressure. The dependence is rather nonlinear. It is also interesting to note that the nonlinearity also appears in the result of the total duration of the dynamic deformation, namely, the duration during which the acceleration of the material is not vanishingly small. This duration for the elastic-plastic problem increases with increasing applied pressure, while, in the elastic case, the duration is a constant as shown in Figure 5. Accordingly, the initiation of slight plastic deformations tend to change considerably the nature of the flow.

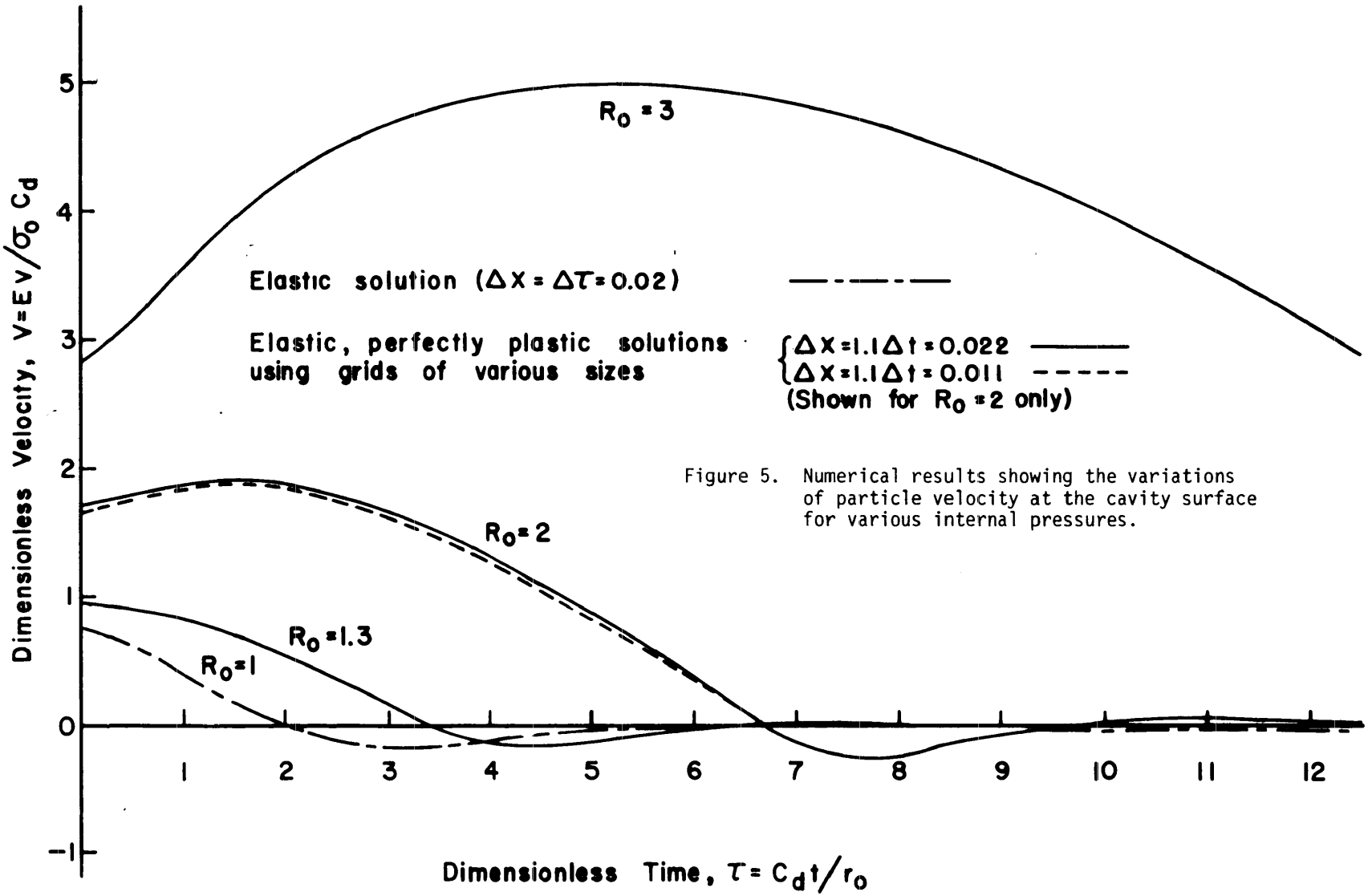

Figure 5. Numerical results showing the variations of particle velocity at the cavity surface for various internal pressures.

6. CONCLUSIONS

It has been shown that the governing equations for an elastic-perfectly-plastic flow with spherical symmetry can be solved through the use of a finite difference technique whose nature is rather well understood in comparison to other similar methods. With a slight modification of the original scheme proposed by Lax, the method can be applied to solve a wide variety of mixed initial-and boundary-value problems involving elastic and plastic flows. The comparison of the results for the dynamic deformation of an elastic cavity obtained using this method and an exact analytical method shows that the accuracy of the numerical solution is acceptable, except probably in the region where a discontinuity in the dependent variables appears. Large errors may occur in this region because of the artificial viscosity added into the equations by using the numerical scheme. Accordingly, for solutions containing discontinuities, an investigation of the error is necessary by varying the grid size and $\Delta x/\Delta \tau$ ratio. If high accuracy is required for the solution near the discontinuities, it is advisable to locate and obtain the discontinuities in the solution using an analytical method as shown by Friedman et al.[4]

For the dynamic expansion of a spherical cavity in an elastic-perfectly-plastic solid, the numerical results for a suddenly applied internal pressure confirm Green's analytical prediction that an elastic-plastic boundary propagates with a constant speed, $c_p = [E/3\rho(1 - 2\nu)]^{1/2}$, when discontinuities in stress and particle velocity occur across the boundary. Within the major duration of an impact the elastic-plastic boundary moves with a variable speed, of which the magnitude cannot be predicted analytically. Therefore, a numerical technique seems to be unavoidable in the investigation of spherical elastic-plastic flow.

The same results have also shown that the quasi-static approximation which is often used in dynamic elasticity may not necessarily hold in dynamic plasticity. The solution for the dynamic problem investigated

does not approach the static solution as a limit when time elapses. This result is probably due to the residual stress produced by the inertia force of the impact.

As far as magnitudes are concerned, the results show a rather nonlinear dependence of the elastic-plastic solution of the internal pressure. This nonlinearity seems to indicate that the nature of the flow would be changed considerably by the initiation of a slight amount of plastic deformation.

ACKNOWLEDGEMENTS

The author wishes to thank Dr. J. T. Frasier of the Exterior Ballistics Laboratory for suggesting the problem, and Mr. T. Addison of the Computing Laboratory for preparing the computer program. The helpful discussions with Mr. Ralph Shear and Mr. J. H. Suckling of the Ballistic Research Laboratories are also greatly appreciated.

REFERENCES

1. H. G. Hopkins, "Dynamic Expansion of Spherical Cavities in Metals," Progress in Solid Mechanics, Volume I, I. N. Sneddon and R. Hill, eds., North-Holland Publishing Co., Amsterdam, page 83, 1960.

2. W. A. Green, "Acceleration Discontinuities At An Elastic/Plastic Loading Surface," Int. J. Engrg. Sci., Volume I, page 523, 1963.

3. N. Davids, P. K. Mehta, and O. T. Johnson, "Spherical Elasto-plastic Waves in Materials," Behavior of Materials Under Dynamic Loading, N. J. Huffington, Jr., ed., ASME, New York, N. Y., page 125, 1965.

4. M. B. Friedman, H. H. Bleich, and R. Parnes, "Spherically Symmetric Elastic-Plastic Shock Propagation," Proc. Amer. Civil Engrs, Volume 91, EM 3 (J. Eng. Mech. Div.) Part I, page 189, 1965.

5. R. Hill, "The Mathematical Theory of Plasticity," Oxford University Press, London, England, page 97, 1964.

6. S. C. Hunter, "The Properties of Spherically Symmetric Disturbances in Ideally Plastic Materials," Proc. Conf. the Properties of Materials at High Rates of Strain, Instn. Mech. Engrs., London, page 147, 1957.

7. P. D. Lax, "Weak Solutions of Nonlinear Hyperbolic Equations and Thier Numerical Computation," Comm. On Pure and Appl. Math., Volume 7, page 159, 1954.

8. S. C. Hunter, "Spherical Symmetric Waves and the Dynamic Response of an Infinite Medium Subjected to Transient Pressure Pulses at an Internal Boundary," Armament Research Establishment Report 49/54, (Ministry of Supply, United Kingdom), December 1954.

9. P. C. Chou and H. A. Koenig, "A Unified Approach to Cylindrical and Spherical Elastic Waves by Method of Characteristics," J. Appl. Mech., Volume 33, page 159m March 1966.

10. L. Roberts, "On The Numerical Solution of the Equations For Spherical Waves of Finite Amplitude, II," J. Math. Phys., page 329, Volume 36, 1958.

11. S. C. Hunter, "Energy Absorbed by Elastic Waves During Impact," J. Mech. Phys. Solids, Volume 5, page 162, 1957.

12. A. E. H. Love, "Mathematical Theory of Elasticity," Dover, New York, page 198, 1944.

APPENDIX

A COMPUTER PROGRAM FOR THE DYNAMIC EXPANSION OF A SPHERICAL CAVITY BY AN INTERNAL PRESSURE (ELASTIC-PERFECTLY-PLASTIC SOLUTION)

The computer program used for obtaining the present results is attached at the end of this Appendix. The program was written in the FORAST language by Mr. T. Addison of the Computing Laboratory. (The reader may consult one of the references at the end of the Appendix for a description of the computer language.) The program can be executed with the BRLESC Computer which is currently being used in the Ballistic Research Laboratories.

The computer program is based on the finite difference schemes described in the main text of this report and will be able to provide information of stress, displacement, and velocity around a spherical cavity which is being expanded by an internal pressure specified with card numbers 157 and 171. The pressure at the boundary is shown as a constant, RR, but can be changed to a function of time, $f(\tau)$; τ is represented by T in the program. The physical quantities R, Θ, V, and U are represented by R, Q, V and U, respectively.

The program can be used for problems with non-vanishing initial values, if the section between cards 13 and 39 is properly modified. This section is now written to represent the similarity solution near $\tau = 0$ for this problem. The similarity solution was put in the program as an alternate way of calculating the results but was omitted in obtaining the final results presented in this report.

The numerical calculation proceeds in increments of time, $\Delta\tau$, while at a given time, τ, it begins with the two data points nearest to the boundary, $x = 1$ and shifts in the positive x direction. Calculations at points other than the boundary point are shown in cards 60 to 79; in cards 60 to 65, the plastic equations are used, and in cards 72 to 79, the elastic equations are applied. Computations at the boundary point occur only once every other time step, as shown in cards 155 to 170 for an elastic case and in cards 171 to 182 for a plastic case.

The input data concerning material properties, specifications for outputs and the dimensions of the grid used for calculations are punched in the two cards at the end of the program which will be read by the machine upon the order written in cards 9 and 11. The input data include the following information:

Program Notations	vs	Physical Quanitites
DX:		Δx
DT:		Δt
DTT:		t of the first output
DTI:		interval of t for output
TMAX:		t of terminating calculation
RR:		Radial stress at the boundary, x = 1
NU		ν
RTO:		initial value of radial stress
A:		$\bar{\sigma}$
TO:		initial time.

The output of the calculation will be stored in a magnetic tape and can be tabulated in a numerical form (cards 112 to 126) as well as plotted in a graphical form (cards 134 to 147). The format of printing is indicated in cards 16 and 17. In plotting, the distributions of stresses, particle velocity and displacement along the radial axis will be presented by color curves in a single graph for each time, t. The size and scaling of the graph is controlled with cards No. 128 and 129. The curves of R, Θ, V and U are all referred to the same scale which is chosen for R, and hence, it is sometimes necessary to adjust the values of V and U with proper numerical factors before plotting, as shown in cards 132 and 149.

```
                                                                                1
                                                                                2
%           MAXT(35) MIN                                                        3
%       MAXO(95000)LINES                                                        4
        BLOC(Y=Y5000)AH1=AH444)U0=U5000)V0=V5000)R0=R5000)Q0=Q5000)              5
        BLOC(I1=I12)D1=D2)                                                      6
        SYN (Y=X1)                                                              7
START   READ=(FW2)=(D1)D2)                                                      8
        READ(DX)DT)DIT)DII)TMAX)RK)                                             9
        ENTER(SET,10)8)0)0)100)                                                10
        READ(NU)X1)RT0)A')T0)                                                  11
        READ=(F1)=(12)NOS.AT(I1)%                                              12
IST     INT(K=1)% INT(KK=I2+1)% X=X1% INT(N=4)% T=T0%                          13
        C2D2=(1=NU=2*NU**2)/(1=NU)% R=RT0% CCCD=SQRT(C2D2)                     14
        CN=(1=NU)/3(1+NU)(1=2*NU)**2% CN=SQRT(CN)                              15
        IF(R(1=NU/(1=NU))> 1)GOTO(3,0)                                         16
1.5     R1,I=RT0% Q1,I=(NU/(1=NU))R% V1,I=- A'*R*C2D2                          17
        MM=1%                                                                  18
        COUNT(5)IN(I)GOTO(1,5)%  INT(M=1)                                      19
        GOTO(PUN)                                                              20
3.0     IF(X>CN*T0)GOTO(4.0)                                                   21
        R1,I=RT0% Q1,I=R1,I-1%                                                 22
        V1,I=-A'((1+NU)-(3(1=NU)**3/(1+NU)(1=2*NU)**2)**.5                     23
    CONT +(3(1=NU)/(1+NU))**.5*R1,I                                            24
        X=X+2*DX% MM=2.0%                    COUNT(5)IN(I)GOTO(3,0)            25
        GOTO(PUN)                                                              26
4.0     R1,I=(1=NU)/(1=2*NU)% Q1,I=NU/(1=2*NU)% V1,I=-(1+NU)A'                 27
        X=X+2*DX% MM=3.0%                                                      28
        COUNT(5)IN(I)GOTO(3,0)                                                 29
PUN     CLEAR(5)NOS.AT(R1)% CLEAR(5)NOS.AT(V1)% CLEAR(5)NOS.AT(Q1)             30
PUN     PUNCH<INITIAL CONDITIONS>% ENTER(PUNCH B)                              31
        PUNCH<                    I          X          V          R      >      32
    CONT<     U          C          I>                                         33
        SET(I=0)J=1)% CC1=D1% CC2=D2                                           34
PUN1    PUNCH=(FW5)=(CC1)CC2)J)X)V1,I)R1,I)Q1,I)J)                             35
        CC1=CC2=0                                                              36
        X=X+2*DX% INC(J=J+1)% COUNT(5)IN(I)GOTO(PUN1)                          37
        SET(I=0)                                                               38
        PUNCH<EJECT PAGE>                                                      39
    COMM  COMPUTE CONSTANTS                                                    40
        CCNU=(1=NU=2*NU**2)                                                    41
        A=1/(1=NU=2*NU*NU)A'% 2DT=1/2*DT% 1N=1=NU                              42
        B11=2DT*1N*A% B12=1/2*DX=1% B21=  NU/DX=1% B23=1 /A*DT                 43
        B31=A(.5*1N/DX=NU)% B32=-2DT                                           44
        A11=2DT% A22=-2DT%  2DX=1/2*DX% A12=A'*C2D2*2DX                        45
        A21=(2DX=1)(1/3*A'(1=2*NU))                                            46
        SET(AY=1)                                                              47
4.1     N1=1% N2=2% I=I+DT  %SET(I=0)                                          48
        INC(K=K+1)                                                             49
        IF=INT(K=2(K/2)) GOTO(EVEN)%                                           50
        VK2=V1% QK2=Q1% RK2=R1 % SET(AY=1)GOTO(4.2)                            51
EVEN    INT(N=N+1)% SET(AY=2)                                                  52
        VK1=V1% QK1=Q1% RK1=R1% QK1=Q1                                         53
4.2     GOTO,AY(AY1)AY2)                                                       54
AY1     XN=X1+N2*DX% N2=N2+2% GOTO(4.5)                                        55
AY2     XN=X1+N1*DX% N1=N1+2                                                   56
4.5     Q1=DT((1=2*NU)(V2,I=V1,I)/2*DX+(NU=.5)(V2,I+V1,I)/XN)/                 57
    CONT CCNU*A'+.5(R2,I+R1,I)=,5(Q2,I+Q1,I)                                   58
        IF=ABS(C1<1. )GOTO(EQ2)                                                59
```

```
      COMM  EQUATION 1  PLASTIC                                                  60
          IV  =DI*A'*C2D2((R2,I-R1,I)/2*DX+2/XN)+(V2,I+V1,I).5                 61
          R1,I=DI((V2,I-V1,I )/2*DX+(V2,I+V1,I )/XN)/3(1-2*NU)A'+               62
      CONT .5(R2,I+R1,I)                                                       63
          Q1,I=R1,I-1                                                          64
          U1,I=(DT(V2,I+V1,I)+U2,I+U1,I).5                                     65
          V1,I=IV                                                              66
          IP2(U5U)(04L)(V1,I)%%   0 GOES TO BIT 9 OF V1                        67
      COMM ZERO GOES TO BIT 9 OF V1=PLASTIC EQ.                                68
          COUNT(N)IN(I)GOTO(4.2)                                               69
          IF-INT(K=2(K/2))GOTO(8.8)% GOTO(BOUND)                               70
      COMM   EQUATION 2  ELASTIC                                               71
EQ2       IV=C2D2*A'*DI((R2,I-R1,I)/2*DX+(R2,I+R1,I-Q2,I-Q1,I)                 72
      CONT /XN)+(V2,I+V1,I).5                                                  73
          R1,I=DI(1N(V2,I-V1,I)/2*DX+NU(V2,I+V1,I)/XN)/(CONU)A'                74
      CONT +.5(R2,I+R1,I)                                                      75
          Q1,I=DI(NU(V2,I-V1,I)/2*DX+(V2,I+V1,I)/2*XN)/CONU*A'                  76
      CONT +.5(Q2,I+Q1,I)                                                      77
          U1,I=(DT(V2,I+V1,I)+U2,I+U1,I).5                                     78
          V1,I=IV                                                              79
          IP2(04L)(04L)(V1,I)%                                                 80
      COMM ONE GOES TO BIT 9 OF V1=ELASTIC EQ.                                 81
          COUNT(N)IN(I)GOTO(4.2)%                                              82
          IF-INT(K=2(K/2))GOTO(8.8)% GOTO(BOUND)                               83
8.8       SET(I=0)J=1)% X=X1% CC1=D1% CC2=D2                                   84
          IF-INT(K> 11) GOTO(9.5)                                              85
          IF-INT(K=2(K/2))GOTO(4.1)                                            86
          PUNCH-(FW1)-< TIME= >T<   CYCLE NO. >(K  )                           87
          ENTER(PUNCH B)                                                       88
          PUNCH<                    I          X          V          R    >    89
      CONT<     Q          U          I>                                       90
9.0       SHX(V1,I)(R8)(MM)                                                    91
      COMM BIT NINE GOES TO BIT ONE                                            92
          B8(MM)(04L)(MM)                                                      93
      COMM BIT ONE ONLY RESULTS IN MM=0 OR 1                                   94
          IP2(U5U)(04L)(V1,I)%%     REPLACES BIT 9                             95
          PUNCH-(FW5)-(CC1)CC2)J)X)V1,I)R1,I)Q1,I)U1,I)MM)                      96
          X=X+2*DX% CC1=CC2=0 % INC(J=J+1)                                     97
          COUNT(N+1)IN(I)GOTO(9.0)% PUNCH<EJECT PAGE>                          98
          GOTO(4.1)                                                            99
          IF-INT-NOT(K=KK)GOTO(10,1)                                          100
9.5       IF-NOT( T=DT1)WITHIN(DT )GOTO(10.1)                                 101
          DT1=DT1+DT1                                                         102
          IF-INT-NOT(K=2(K/2))GOTO(PUN1 )                                     103
          CC1=CC2=0% X=X+DX                                                   104
          PUNCH-(FW1)-< TIME= >T<   CYCLE NO. >(K  )                          105
          ENTER(PUNCH B)                                                      106
          PUNCH<                         X          V          R    >       107
      CONT<     Q          U          I>                                      108
8.9       SHX(V1,I)(R8)(MM)                                                   109
          B8(MM)(04L)(MM)                                                     110
          IP2(U5U)(04L)(V1,I)                                                 111
          PUNCH-(FW5)-(CC1)CC2)J)X)V1,I)R1,I)Q1,I)U1,I)MM)                     112
          X=X+2*DX% INC(J=J+1)                                                113
          COUNT(N  )IN(I)GOTO(8.9)% GOTO(PEP)                                 114
          INT(KK=KK+12)                                                       115
PUN1      PUNCH-(FW1)-< TIME= >T< CYCLE NO. >(K   )% ENTER(PUNCH B)           116
          PUNCH<                    I          X          V          R    >    117
      CONT<     Q          U          I>                                      118
9.7       SHX(V1,I)(R8)(MM)                                                   119
```

```
        COMM BIT NINE GOES TO BIT ONE                                          140
             B8(MM)(04L)(MM)                                                   141
        COMM BIT ONE ONLY RESULTS IN MM=0 OR 1                                 142
             IP2(050)(04L)(V1,I)%%      REPLACES BIT 9                         143
             PUNCH=(FW5)=(CC1)CC2)J)X)V1,I)R1,I)Q1,I)U1,I)MM)                   144
             X=X+2*DX% CC1=CC2=0 % INC(J=J+1)                                  145
             COUNT(N+1)IN(I)GOTO(9,7)%                                         146
PEP          PUNCH<EJECT PAGE>                                                 147
             XMAX=14.0% RMAX=15.% XMIN=1.0% RMIN=-4.5                          148
             RX=RS=RMAX/10% XX=XS=(XMAX-XMIN)/26                               149
6.60         SET(I=0)%                                                         150
             Y=X1                                                              151
6.61         V1,I=-V1,I/5.0% Y1,I=Y,I+2*DX% U1,I=-U1,I/200.                    152
             COUNT(N+1)IN(I)GOTO(6.61)                                         153
             GOTO,BY(AY5)(AY6)(AY3)(AY4)                                       154
AY5          SET(XB=4)(YB=14)%                                                 155
AY7          INC(BY=BY+1)GOTO(9.8)                                             156
AY6          SET(XB=31)GOTO(AY7)                                               157
AY3          SET(YB=42)GOTO(AY7)                                               158
AY4          SET(XB=4)(BY=1)%                                                  159
9.8     STOR                                                                   160
             PUNCH<XB= >XB < YB= >YB                                           161
             ENTER(PLOT.S)1),XB),YB)Q51)Q50)XS)RS)AH1))                        162
             ENTER(PLOT.D)1)1)1)3)Y)Q1),I)                                     163
             ENTER(PLOT.D)1)1)1)4)Y)R1),I)                                     164
             ENTER(PLOT.D)1)1)1)5)Y)U1),I)                                     165
             ENTER(PLOT.D)1)1)1)6)Y)V1),I)                                     166
             ENTER(PLOT.A)1)XX)RX)XMIN)XMAX)RMIN)RMAX)                         167
             SET(I=0)                                                          168
6.62         V1,I=-V1,I*5.0% U1,I=-U1,I*500                                    169
             COUNT(N+1)IN(I)GOTO(6.62)                                         170
9.9          IF-INT(BY>1)GOTO(10.1)% ENTER(PLOT.F)1)                           171
10.1         IF(T>TMAX)GOTO(NPROB)                                             172
             IF-INT(K=15)GOTO(NPROB)% GOTO(4.1)                                173
NPROB        ENTER(ENDPLOT))1)% GOTO(N.PROB)                                   174
BOND         SET(I=0)                                                          175
             B14=2DT*1N*A*VK1+(.5/DX+1)RK2-QK1                                 176
             R0=RK                                                             177
             B24=QK1/A*DT+2*NU*VK2/DX-(NU/DX-1)VK1                             178
             B34=-R0/DT+2DT*RK2+A(1N*VK2/DX-(.5*1N/DX-NU)VK1)                  179
             V0 =(B32(B23*B14-B24)-B34*B23*B12)    /(B32(B23*B11-B21)          180
        CONT -B31*B23*B12)                                                     181
             Q0  =(B24-B21*V0)/B23                                             182
             IF-ABS(R0-Q0>1 )GOTO(BOND1)                                       183
             U0=(V0+VK1)DT+UK1                                                 184
             MOVE(N)NOS.FROM(V0,N/-1)TO (V1,N/-1)                              185
             MOVE(N)NOS.FROM(R0,N/-1)TO (R1,N/-1)                              186
             MOVE(N)NOS.FROM(Q0,N/-1)TO (Q1,N/-1)                              187
             MOVE(N)NOS.FROM(U0,N/-1)TO(U1,N/-1)                               188
             V1=V0% Q1=Q0% R1=R0% U1=U0                                        189
             GOTO(8.8)                                                         190
BOND1        R0=RK                                                             191
             A23=-(R0-.5*RK2)/DT+(VK2/DX=(2DX-1)VK1)/5*A'(1-2*NU)              192
             A13=2DT*VK1+A'*C2D2(2DX*RK2+2)                                    193
             V0  =(A22*A13-A12*A23)/(A11*A22-A21*A12)                          194
             Q0=R0-1                                                           195
             U0=(V0+VK1)DT+UK1                                                 196
             MOVE(N)NOS.FROM(V0,N/-1)TO (V1,N/-1)                              197
             MOVE(N)NOS.FROM(R0,N/-1)TO (R1,N/-1)                              198
             MOVE(N)NOS.FROM(Q0,N/-1)TO (Q1,N/-1)                              199
```

```
          MOVE(N)NOS.FROM(U0,N/-1)TO(U1,N/-1)                                  100
          V1=V0% Q1=Q0% R1=R0% U1=U0                                           101
          GOTO(8.8)                                                            102
F1    FORM(4-6)1-12)                                                           103
FW1   FORM(12-10)4-6)                                                          104
FF    FORM (12-6)3-1)1-10)                                                     105
FW2   FORM(8-10)8-10)                                                          106
FW5   FORM(8-10)8-4)4-6)3-2)1-1)12-10)3-1)1-5)4-6)                             107
      LIST                                                                     108
      END GOTO(START)                                                          109
BOUNDARY P1,
 .011        .01          .25          .25          15.0          2.0
 30000000 00 10000000 01 0.10         1.000000000
             50000
      PROB
```

REFERENCES

1. M. J. Romanelli, "Introductory Programming for ORDVAC and BRLESC," FORAST (Formula and Assembly Translator), Ballistic Research Laboratories Report No. 1209, July 1963.

2. L. W. Campbell and G. A. Beck, "The FORAST Programming Language for ORDVAC and BRLESC (Revised)," Ballistic Research Laboratories Report No. 1273, March 1965. (Supersedes Report No. 1172).

DISTRIBUTION LIST

No. of Copies	Organization
20	Commander Defense Documentation Center ATTN: TIPCR Cameron Station Alexandria, Virginia 22314
1	Commanding General U.S. Army Materiel Command ATTN: AMCRD-TE Washington, D.C. 20315
1	Commanding General U.S. Army Missile Command ATTN: AMSMI-AML Redstone Arsenal, Alabama 35809
1	Commanding Officer U.S. Army Engineer Research & Development Laboratories ATTN: STINFO Div Fort Belvoir, Virginia 22060
1	Commanding Officer U.S. Army Picatinny Arsenal ATTN: SMUPA-VA6 Dover, New Jersey 07801
1	Commanding General U.S. Army Weapons Command Rock Island, Illinois 61202
1	Commanding Officer U.S. Army Rock Island Arsenal Rock Island, Illinois 61202
1	Commanding Officer U.S. Army Materials Research Agency Watertown, Massachusetts 02172
1	Commanding Officer U.S. Army Research Office (Durham) Box CM, Duke Station Durham, North Carolina 27706
3	Commander U.S. Naval Air Systems Command Headquarters ATTN: AIR-604 Washington, D.C. 20360
1	Commander U.S. Naval Ordnance Laboratory Silver Spring, Maryland 20910
1	Superintendent U.S. Naval Postgraduate School ATTN: Tech Rept Sec Monterey, California 93940
1	Director U.S. Naval Research Laboratory Washington, D.C. 20390
1	Commander U.S. Naval Weapons Laboratory ATTN: Tech Lib, MAL Dahlgren, Virginia 22448
1	RTD (RTTM) Bolling AFB, D.C. 20332
1	AFML (MAA) Wright-Patterson AFB Ohio 45433
1	ARL (ARM, Mr. H. Fettis) Wright-Patterson AFB Ohio 45433
1	Sandia Corporation ATTN: Org 1115, Dr. C. Karnes P.O. Box 5800 Albuquerque, New Mexico 87115
1	Sandia Corporation Livermore Laboratory ATTN: Dr. S. Chiu P.O. Box 969 Livermore, California 94550

DISTRIBUTION LIST

No. of Copies	Organization
2	General Electric Company Space Sciences Laboratory ATTN: Dr. F. Wendt Dr. J. Heyda Dr. T. Riney P. O. Box 8555 Philadelphia, Pa. 19101
3	Brown University Division of Engineering ATTN: Prof P. Symonds Prof J. Duffy Prof D. Drucker Providence, Rhode Island 02912
3	Brown University Division of Engineering ATTN: Prof H. Kolsky Prof R. Clifton Prof W. Green Providence, Rhode Island 02912
2	Cornell University Department of Theoretical & Applied Mechanics ATTN: Prof D. Robinson Prof R. Lance Ithaca, New York 14850
3	The University of Texas Department of Engineering Mechanics ATTN: Prof E. Ripperger Prof H. Calvit Prof C. Yew Austin, Texas 78758
1	Professor J. Bell Department of Engineering Mechanics The Johns Hopkins University 34th and Charles Street Baltimore, Maryland 21218
1	Professor H. Bleich Institute of Flight Structures Columbia University New York, New York 10027
1	Professor P. C. Chou Department of Aeronautical Engineering Drexel Institute of Technology 32nd and Chestnut Streets Philadelphia, Pa. 19104
1	Professor N. Davids Department of Engineering Mechanics Pennsylvania State University 319 Electrical Engineering East University Park, Pa. 16802
1	Professor W. Goldsmith Department of Engineering Mechanics University of California Berkeley, California 94704
1	Professor P. D. Lax Courant Institute of Mathematical Sciences New York University 251 Mercer Street New York, New York 10012
1	Professor E. H. Lee Department of Engineering Mechanics Stanford University Palo Alto, California 94304
1	Professor L. Malvern College of Engineering Michigan State University East Lansing, Michigan 48823

DISTRIBUTION LIST

No. of Copies	Organization
1	Professor W. Prager University of California 8602 La Jolla Shores Drive La Jolla, California 92037
1	Professor T. Ting Department of Materials Engineering University of Chicago Chicago, Illinois 60637
1	Dr. T. D. Dudderar Bell Telephone Laboratory Mountain Avenue Murray Hill, New Jersey 07971
1	Dr. U. Lindholm Department of Mechanical Sciences Southeast Research Institute 8500 Culebra Road San Antonio, Texas 78228
1	Dr. R. Sedney Research Institute for Advanced Studies The Martin Company 7212 Bellona Avenue Ruxton, Maryland 21212
	Aberdeen Proving Ground
	Ch, Tech Lib
	Air Force Ln Ofc Marine Corps Ln Ofc Navy Ln Ofc CDC Ln Ofc

Unclassified
Security Classification

DOCUMENT CONTROL DATA - R & D

(Security classification of title, body of abstract and indexing annotation must be entered when the overall report is classified)

1. ORIGINATING ACTIVITY (Corporate author)	2a. REPORT SECURITY CLASSIFICATION
U.S. Army Ballistic Research Laboratories Aberdeen Proving Ground, Maryland	Unclassified
	2b. GROUP

3. REPORT TITLE

THE DYNAMIC EXPANSION OF A SPHERICAL CAVITY IN AN ELASTIC-PERFECTLY-PLASTIC MATERIAL

4. DESCRIPTIVE NOTES (Type of report and inclusive dates)

5. AUTHOR(S) (First name, middle initial, last name)

Mok, Chi-Hung

6. REPORT DATE	7a. TOTAL NO. OF PAGES	7b. NO. OF REFS
February 1967	41	14

8a. CONTRACT OR GRANT NO.	9a. ORIGINATOR'S REPORT NUMBER(S)
b. PROJECT NO. RDT&E 1P222901A201	Report No. 1357
c.	9b. OTHER REPORT NO(S) (Any other numbers that may be assigned this report)
d.	

10. DISTRIBUTION STATEMENT

Distribution of this document is unlimited.

11. SUPPLEMENTARY NOTES	12. SPONSORING MILITARY ACTIVITY
	U.S. Army Materiel Command Washington, D.C.

13. ABSTRACT

It has been shown that a finite-difference numerical technique can be used to solve mixed initial-and boundary-value problems involving high-speed elastic-plastic flow with spherical symmetry. Numerical solutions for the dynamic expansion of a spherical cavity under a constant pressure are presented to demonstrate the nature and capability of the numerical scheme. The solution for an elastic material agrees closely with the exact solution. The solution for an elastic-perfectly-plastic material has confirmed Green's prediction concerning the motion of the elastic-plastic boundary. At large times, the asymptotic solution of the dynamic problem is different from the quasi-static solution. This result indicates that the quasi-static approximation may not hold in dynamic plasticity. A non-linear dependence of the plastic solution on the boundary condition is also observed in the results.

DD FORM 1 NOV 68 1473 REPLACES DD FORM 1473, 1 JAN 64, WHICH IS OBSOLETE FOR ARMY USE.

Unclassified
Security Classification

14. KEY WORDS	LINK A		LINK B		LINK C	
	ROLE	WT	ROLE	WT	ROLE	WT
Dynamic Plasticity Expansion of Spherical Cavity Lax Computation Scheme Elastic-Perfectly-Plastic Material						